J Mol Model (2012) 18:2917–2927
DOI 10.1007/s00894-011-1310-2

ORIGINAL PAPER

Large-scale virtual screening for the identification of new *Helicobacter pylori* urease inhibitor scaffolds

Homa Azizian · Farzaneh Nabati · Amirhossein Sharifi · Farideh Siavoshi · Mohammad Mahdavi · Massoud Amanlou

Received: 18 May 2011 / Accepted: 14 November 2011 / Published online: 3 December 2011

Abstract Here, we report a structure-based virtual screening of the ZINC database (containing about five million compounds) by computational docking and the analysis of docking energy calculations followed by in vitro screening against *H. pylori* urease enzyme. One of the compounds selected showed urease inhibition in the low micromolar range. Barbituric acid and compounds **1a, 1d, 1e, 1f, 1g, 1h** were found to be more potent urease inhibitors than the standard inhibitor hydroxyurea, yielding IC_{50} values of 41.6, 83.3, 66.6, 50, 58.8, and 60 μM, respectively (IC_{50} of hydroxyurea = 100 μM). 5-Benzylidene barbituric acid has enhanced biological activities compared to barbituric acid. Furthermore, the results indicated that among the substituted 5-benzylidene barbiturates, those with *para* substitution have higher urease inhibitor activities. This may be because the barbituric acid moiety is closer to the bimetallic nickel center in unsubstituted or *para*-substituted than in *ortho*- or *meta*-substituted analogs, so it has greater chelating ability.

Keywords *Helicobacter pylori* · Urease inhibitors · Virtual screening · 5-Benzylidene barbituric acid · Docking

H. Azizian · F. Nabati · A. Sharifi · M. Mahdavi · M. Amanlou (✉)
Department of Medicinal Chemistry, Faculty of Pharmacy and Pharmaceutical Sciences Research Center,
Tehran University of Medical Sciences,
16 Azar Ave.,
Tehran, Iran
e-mail: amanlou@tums.ac.ir

F. Siavoshi
Department of Microbiology, Faculty of Sciences,
University of Tehran,
Tehran, Iran

M. Amanlou
Drug Design and Development Research Center,
Tehran University of Medical Sciences,
16 Azar Ave.,
Tehran, Iran

Introduction

Helicobacter pylori (*H. pylori*) is a Gram-negative microaerophilic bacterium that infects up to 50% of the world's human population [1]. Gastric disorders, including gastritis, ulceration, and the most severe gastric carcinomas and primary gastric lymphomas are etiologically connected with *Helicobacter* species infections [2].

H. pylori urease (E.C. 3.5.1.5) is a nickel-dependent amidohydrolase which catalyzes urea decomposition into ammonia and carbon dioxide, with carbamate as the intermediate [3]. Urease is known to be a major cause of pathologies induced by *H. pylori*, as its ureolytic activity allows these pathogens to overcome acidic pH (part of the natural defense system at stomach mucosal surfaces), thus enabling them to colonize bacteria in the mucus layer [4, 5].

While plant and fungal ureases are known to mostly be homohexamers (α_6), bacterial ureases are typically heterotrimers $(\alpha\beta\gamma)_3$ consisting of three distinct subunits, one large (α, 60–76 kDa) and two small (β, 8–21 kDa; and δ, 6–14 kDa) [6]. However, *H. pylori* urease is an exception, as it is composed of only two subunits, which form a dodecameric complex $((\alpha\beta)_3)_4$ [7]. Importantly, in all known ureases, the active site is always located in the α subunit and contains a binuclear nickel center, with Ni–Ni distances that range between 3.5 and 3.7 Å [8].

High-throughput virtual screening (HTVS) is a technique that can screen millions of compounds rapidly, reliably, and cost-effectively. Virtual screening (VS) involves computationally screening very large chemical libraries of commercially available chemicals for compounds that complement a target of known structure, and then experimentally testing the compounds with the highest predicted binding energies [9]. Since the crystal structure of *H. pylori* urease has been published [7], VS can be performed by the structure-based virtual screening (SBVS) method, which utilizes virtual docking to develop new compounds that can be used for *H. pylori* urease inhibition. In our case, the target structure was *H. pylori* urease in complex with acetohydroxamic acid (AHA) (PDB code 1E9Y), which was retrieved from the Protein Data Bank [7].

Many urease inhibitors have been investigated in the past decades, such as phosphorodiamidates, hydroxamic acid derivatives, and imidazoles [10], but most of these compounds are too toxic or unstable to allow their use in vivo. Thus, the search is still on for novel urease inhibitors with promising levels of activity.

In continuation of our efforts to study arginase as a potential target for *H. pylori* growth inhibition [11], we employed an integrated database screening strategy involving protein structure-based molecular docking simulation of the urease–inhibitor complex by the Autodock suite. We describe that work below.

Methods and materials

Target preparation

The structure of *H. pylori* urease (in complex with acetohydroxamic acid) was retrieved from the Protein Data Bank (PDB ID; 1E9Z) [7]. In the first step of our study, all of the water molecules and co-crystallized ligands were removed. The initial parameters of Ni were set to r=1.170 Å, q=+2.0, and a van der Waals well depth of 0.100 kcal mol^{-1} [12]. The pK_a values of the residues in the enzyme were calculated to determine if any of them were likely to adopt nonstandard ionization states, using PROPKA 2.0 [13]. The side chains of the lysine, arginine, and histidine residues were protonated, while the carboxylic groups of glutamic acid and aspartic acid were deprotonated.

Description of the active site of *H. pylori* urease

The active site of *H. pylori* urease is shown in Fig. 1. The Ni^{2+}–Ni^{2+} distance is 3.4 Å [8]. These two Ni^{2+} ions are bridged by a carbamylated lysine (KCX) through its O atoms. One of the Ni^{2+} ions is coordinated by H221 (NE2), H248 (ND1), H274 (NE2), and KCX219 (OQ1), and the other is coordinated by H136 (NE2), H138 (NE2), KCX219 (OQ2), and D362 (OD2). According to crystallographic studies of the urease–AHA complex, A169 acts as a hydrogen-bond acceptor at the active site. In addition, there are two residues at the bottom of the active site (C321 and R338) that can form a hydrogen bond and/or undergo a polar interaction with the ligand.

Compound database selection

We chose to use the ZINC 8 library [14], because ZINC is an open-source database. Using the application of Lipinski's "rule of five" [15] (molecular weight <500, partition coefficient log$P$ <5, number of H-bond donors <5, number of H-bond acceptors <10, and number of rotatable bonds <7), a total of 737,685 compounds were retrieved from the Clean Lead category of the ZINC 8 database, from which reactive groups such as SO_2Cl and SO_2F are omitted.

Strategies used during the filtering process

A variety of filters were applied to the hits obtained from the database: ligand docking, binding affinity estimation, the presence of active site pocket interactions with specific residues, the presence of key interactions, and the presence of a lower binding energy than that of AHA. Furthermore, we implemented visual inspection and selected one compound from each class of scaffolds. The best hits from this search were tested for inhibition experimentally.

Figure 2 shows the VS flowchart we employed in this study:

1. Compound libraries used in the VS experiments were first filtered to remove reactive but specious groups and unsuitable compounds that would not pass clinical trials based on Lipinski's rule of five. From the 5,000,000 compounds present in the ZINC 8 database, 737,685 druglike compounds were retrieved from the Clean Lead category of ZINC 8.
2. Following the docking procedure, the best 100,000 compounds were selected based on binding affinity, using Autodock 3.0.5.
3. Visualization of the docking solutions showed that, although some compounds possessed high scores (low docking energies), they were relatively far away from the center of the binding pocket. As we were looking for competitive inhibitors, the ideal compounds are those that fit well within the binding pocket. The following residues were considered to be significant in the binding pocket of *H. pylori* urease: H221, H248, H274, KCX219, H136, H138, D362, R338, C322, and the two Ni^{2+} ions. For the process of selecting compounds that undergo interactions with

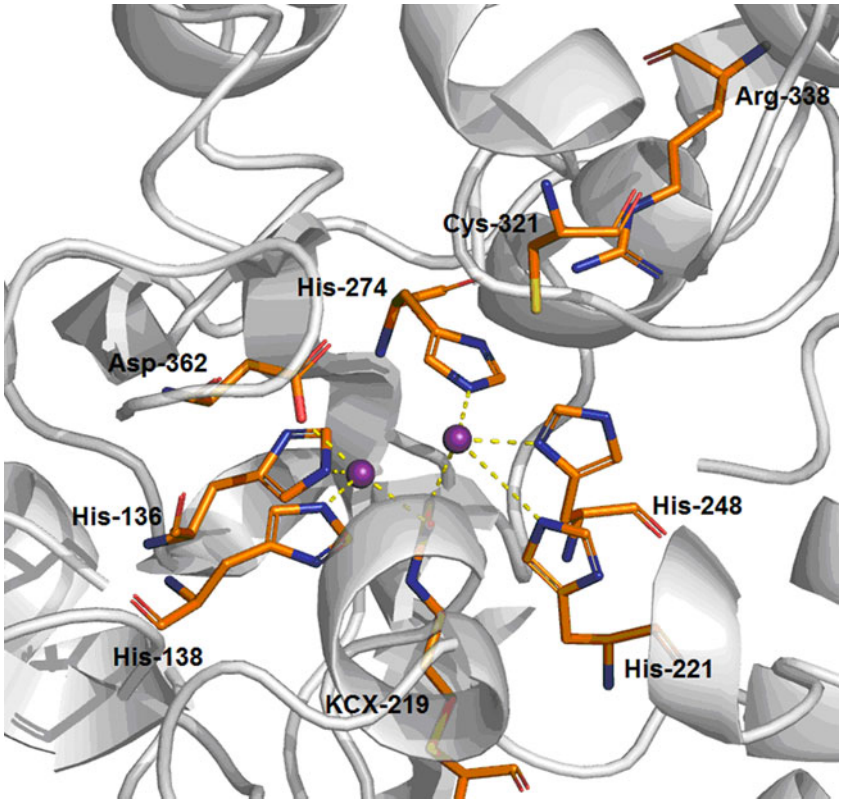

Fig. 1 3D representation of the active site of *H. pylori* urease

the abovementioned residues, we prepared an in-house script (just as we did for the automated docking step) that defined the hydrophobic interactions and hydrogen bonds between the docked ligand and the surrounding residues that were closer than 3 Å. Compounds that were not within the binding pocket were rejected; about 15,000 compounds were left.

4. To further filter these compounds, those with binding energies lower than that of AHA were omitted, as we were seeking compounds with a higher potential to bind at the *H. pylori* urease active site. After filtering in this manner, 1000 compounds remained.
5. "Good-looking" conformations were then chosen, which led to 500 hits. The criteria for such good-looking conformations were:
   a. A chemical match between the atoms in the ligand conformer and those in the receptor. For example, the carbon atoms in the ligand should be close to hydrophobic atoms in the receptor, while nitrogens and oxygens in the ligand should be near to similar atoms in the binding pocket.
   b. Charge complementarity.
   c. Other particular aspects of our system. We know that the active site of urease contains a binuclear nickel center that is necessary for the enzymatic action of the urease. Urea binds to the more electrophilic Ni(1) ion through the oxygen atom of its carbonyl group, making the carbonyl carbon more electrophilic and hence more susceptible to nucleophilic attack. Thus, by visual inspection, we examined how the ligand's conformers interacted with the Ni ions. Some compounds showed metal coordination far from the nickel ions, thus decreasing the tendency of these compounds to coordinate, while some compounds coordinated closer to the bimetallic nickel center.
6. One hundred twenty scaffolds were classified based on structural diversity.
7. Finally, three compounds were chosen based on their availability/synthetic accessibility.

Automated docking approach

Autodock 3.0.5 [16], which uses a stochastic search based algorithm, was used for the docking study. AutoDockTools 1.5.2 (ADT) [17] was used to merge nonpolar hydrogens, add Gasteiger charges, set up rotatable bonds for each ligand, and assign Kollman charges to the enzyme via AutoTors [16]. This produced the corresponding pdbq file required by Autodock. A grid box was created around the active site to evaluate the ligand–protein interaction, and grid maps for each atom type and an electrostatic map of the ligand at each point in the docking simulation were also

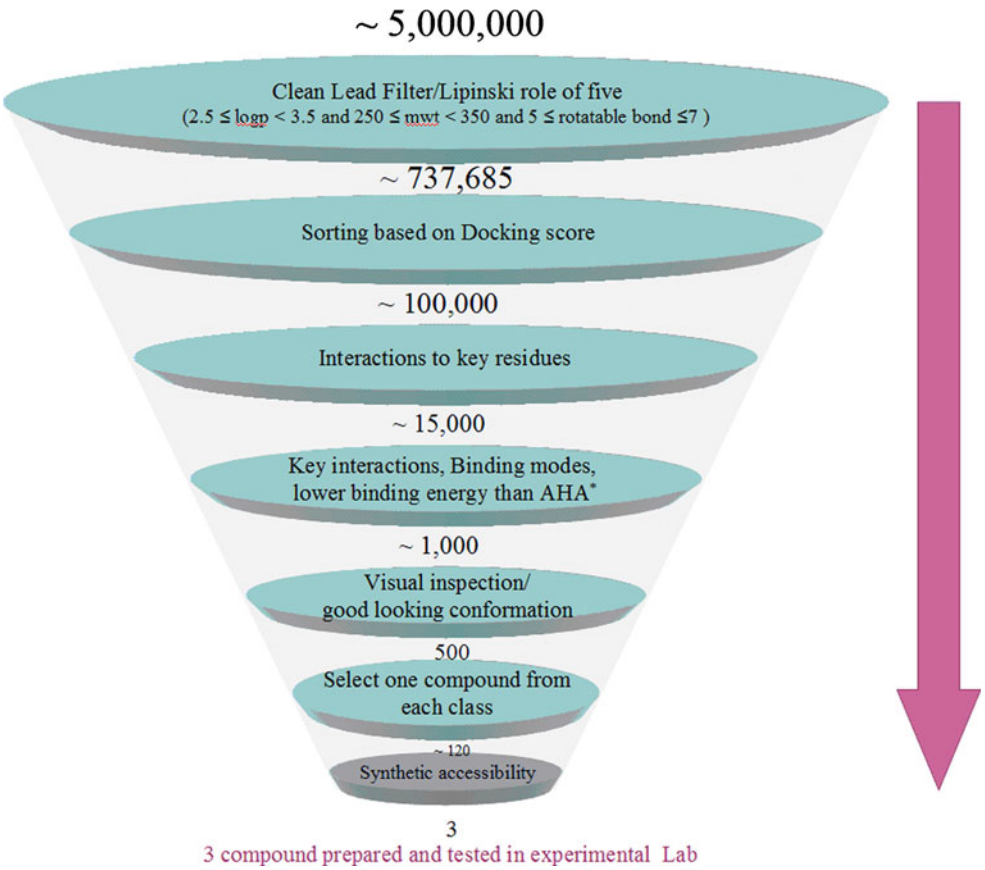

Fig. 2 Representation of the overall filtering process. The process started with 5,000,000 compounds, and at different stages various filters were applied as indicated in the figure in order to reduce false positives and finally to identify the best possible hits, which are more likely to be leads

obtained. The volume of the grid box should be large enough to allow the ligand to rotate freely. In Autodock, the initial files were constructed by ADT, and grid calculation was performed by Autogrid [16]. The grid spacing was 0.375 nm in each dimension, and each grid map consisted of 40×40×40 Å points around the active site. The center of the grid was set to the average coordinates of the two Ni^{2+} ions in the α chain of *H. pylori* urease. A Lamarckian genetic algorithm (LGA) was used for the conformational search. Each Lamarckian job consisted of 250 runs. The initial population was 150 structures, and the maximum number of energy evaluations and generations was 2.5×10^7. The other parameters were set to default values. The final structures were clustered and ranked according to the most favorable docking energy. Docking energy is the algebraic sum of the nonbonded and electrostatic energies along with the internal free energy of the ligand. This was calculated as the difference between the total complex energy and those of its components, and it represents the gain in potential energy due to interactions between the molecules that form the complex. Van der Waals and hydrogen bonding was included in the calculated nonbonded energy.

Clustering was performed by the Autodock program, and runs with same conformations were put in the same clusters. Autodock performed the clustering by first sorting all of the docked conformations from lowest energy (best docking) to highest. The best overall docked conformation was used as the seed for the first cluster. Then the coordinates of the second best conformation were compared with those of the best to calculate the root mean square deviation between the two conformations. If the calculated RMS value was smaller than the specified cutoff (0.5 by default), that conformation

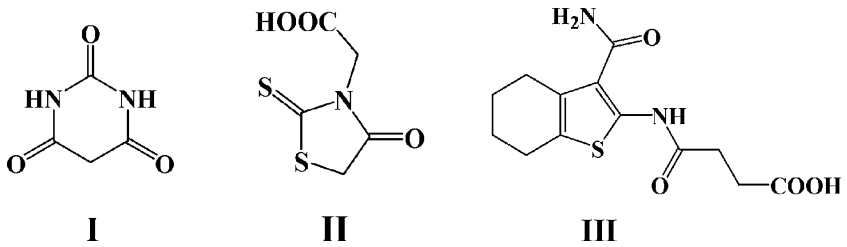

Fig. 3 Three compounds selected by virtual screening: *I* barbituric acid, *II* thiazolidine, *III* tetrahydrobenzothiophen derivatives

Table 1 Percent urease inhibitions of selected virtual screening compounds at concentrations of 1 mM

Compound	% Inhibition (1 mM)
Barbituric acid	76
Thiazolidine	ppt
Tetrahydrobenzothiophen	ppt
Hydroxyurea*	60

ppt precipitated in the reaction mixture at the concentration used

* Used as positive control, standard urease inhibitor

was added to the bin containing the best conformation. If it was not, the second best conformation became the reference for a second bin. Then the RMS between the third conformation and the best conformation was computed, and if they were close enough it was added to the first bin. If not, it was compared with the seed for the second bin, and so on [16].

The top-ranked conformation of each ligand was selected. All docking procedures, from preparing input files to analyzing results, were performed automatically by scripts written in-house.

Computational resources

The computational studies were carried out on a computer cluster comprising four sets of HP Prolient ML370-G5 tower servers equipped with two quad-core Intel Xeon E5355 processors (2.66 GHz) and 4 GB of RAM, running a Linux platform (Suse 10.2).

Urease inhibition assay

The enzyme assay was performed by the Berthelot alkaline phenol–hypochlorite method. This method is based on the release of ammonia (NH_3), which reacts with hypochlorite (OCl^-) to form a monochloramine [18, 19]. This product then reacts with phenol to form blue-colored indophenols whose absorbance is measured at 625 nm. In brief, 10 μl of enzyme solution were incubated with 140 μl of urea and 5 μl of inhibitor at a final concentration of 25 mM in phosphate buffer solution (pH 7.6, 100 mM) for 15 min at 37 °C. The ammonia liberated was estimated using 500 μl of solution A (containing 5.0 g phenol and 25 mg of sodium nitroprusside) and 500 μl of solution B [containing 2.5 g sodium hydroxide and 4.2 ml of sodium hypochlorite (5% chlorine) in 500 ml of distilled water] at 37°C for 30 min, and the absorbance was measured at 625 nm against the control.

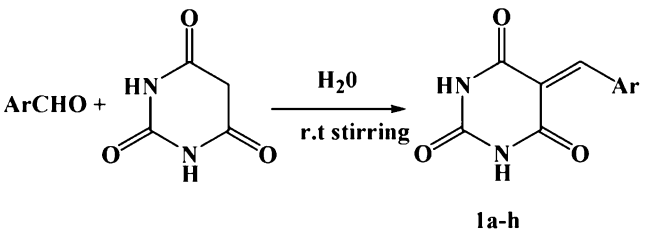

Scheme 1 Synthesis of 5-benzylidene barbituric acid derivatives

Results and discussion

Reliability of the docking protocol

Before investigating a large library of compounds using VS, the reliability of the applied docking protocol was assessed by re-docking acetohydroxamic acid (AHA) into the active site of the *H. pylori* urease. The key characteristic of a good docking program is its ability to reproduce the experimental or crystallographic binding modes of ligands. To test this, a ligand is taken out of the X-ray structure of its protein–ligand complex and re-docked into its binding site. The docked binding mode is then compared with the experimental binding mode, and the RMSD is calculated; a prediction of a binding mode is considered successful if the RMSD is below a certain value (usually<2.0 Å). The RMSD between the docked binding mode and the experimental binding mode for AHA when docked into the *H. pylori* urease was within this cutoff limit (1.42 Å). This protocol was then similarly applied to all compound libraries.

Compound selection and biological activities

After the aforementioned criteria had been applied, three structurally distinct compounds (Fig. 3) were submitted for in vitro screening against urease inhibition by the Weatherburn urease assay method [18]. Percentage inhibitions at 1 mM concentrations of the selected compounds were initially determined from the formula $100 - (OD_{\text{test well}}/OD_{\text{control}}) \times 100$. Hydroxyurea was used as the standard inhibitor of urease. The results are reported in Table 1.

The compound thiazolidine was obtained commercially from Merck. As we were not able to obtain the two other compounds due to them being unavailable to us during the present study, barbituric acid and tetrahydrobenzothiophen derivatives were synthesized using previously reported methods and investigated further [20, 21].

Barbituric acid showed good urease inhibitory activity, with a percent urease inhibition of 76, as shown in Table 1.

Although the tetrahydrobenzothiophen derivatives and thiazolidine showed acceptable interactions with the active site of *H. pylori* urease, they were precipitated in Weatherburn's assay medium. Interestingly, the tetrahydrobenzothiophen derivatives (Fig. 3 III) resemble 2-aminothiophen derivatives, which were recently found to be urease inhibitors by Khan et al. [22].

Table 2 Urease inhibitory activities (IC_{50}±SEM in μM) and interaction energies (kcal mol^{-1}) of 5-benzylidine barbiturate derivatives

Compound	Ar	Docking energy (kcal/mol)	IC_{50}±SEM (μM)
1a	C_6H_5	−9.47	41.6 ±4.82
1b	2-(OH)-C_6H_4	−6.53	116.6 ±4.48
1c	2-(NO_2)-C_6H_4	−6.31	ppt
1d	3-(NO_2)-C_6H_4	−6.48	83.3 ±3.01
1e	4-(Cl)-C_6H_4	−7.44	66.6 ±2.32
1f	4-(OCH_3)-C_6H_4	−7.47	50 ±5.71
1g	3-(OH)-4-(OCH_3)-C_6H_3	−7.63	ppt
1h	4-(F)-C_6H_4	−7.54	55.8 ±2.75
Barbituric acid	–	−6.82	60 ±4.93
Hydroxyurea	–	−5.50	100 ±3.03
AHA	–	−4.44	ND

Values given are means±SEM of three observations. *ppt* precipitated in the reaction mixture at the concentration used, *ND* not determined

The structure–activity relationship for barbiturate derivatives

To optimize the ligand interactions with the binding site, we decided to investigate different derivatives of barbituric acid (**1a–h**). The synthesis of some 5-benzylidene barbituric acid derivatives (**1a–h**) was carried out based on a previously reported uncatalyzed Knoevenagel condensation [20]. Scheme 1 presents the general synthesis of these compounds. All synthetic compounds were then submitted for biological screening against urease inhibition, after which binding energy calculations were performed to analyze the quality of the binding mode using the docking method (Table 2).

Table 2 shows that the 5-benzylidene barbiturate derivatives are more potent than the standard inhibitor of urease, hydroxyurea (IC_{50} value of 100 μM). The synthesized compounds can be regarded as substrate-like inhibitors based on their structural similarity to the natural substrate of urease, urea (Fig. 4). The results revealed that the aryl parts of the test compounds play a significant role in their activity. The most active compound, 5-benzylidene barbituric acid (**1a**) (IC_{50}=41.6±4.82 μM), has no substituent on the aryl moiety, meaning that it is less polar than other substituted structures.

Compounds with a substituent at the *para* position were found to be good inhibitors of urease (**1f**, **1h**, **1e**; IC_{50} =50± 5.71, 55.8±2.75, 66.6±2.32 μM, respectively), whereas compounds **1d** and **1b**, with the substituent at the *meta* and *ortho* positions, respectively, had lower activities (IC_{50} =83.3±3.01 and 116.6±4.48 μM, respectively), indicating that the position of the substituent influences the inhibitory activity. The corresponding *ortho*-nitro- (**1c**) and 3-hydroxy-4-methoxysubstituted (**1g**) compounds were found to precipitate at the concentration used.

Generally, *para*-substituted 5-benzylidene barbiturate exhibited good inhibitory activity against *H. pylori* urease (Table 2), which attracted us to them as potential lead compounds for new *H. pylori* urease inhibitors.

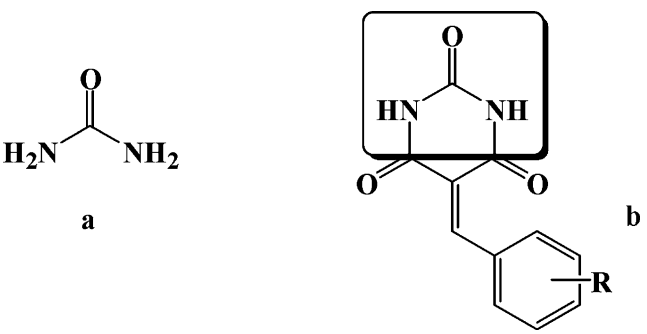

Fig. 4 Representation of the possible binding mode to urease. **a** Natural substrate of urease: urea. **b** Substituted 5-benzylidene barbiturate

Investigating the binding modes of the active compounds

The binding mode of barbituric acid suggested that it fitted well into the urease binding pocket (Fig. 5a). The α-carbon, which has a reactive acidic hydrogen atom, orients toward D362 (COO–), A365 (C=O) and H138 (NE), and one of the adjacent carbonyls orients towards the two Ni^{2+} ions. D362, A365, and H138 have the potential to abstract the α-carbon's acidic hydrogen and produce an ionizable barbituric ring. The resulting carbanion is stabilized to a considerable degree due to the additional aromatic delocalization of negative charge (Fig. 6). Thus, we can propose that the carbonyls adjacent to the α-carbon have the potential to change to hydroxyls as a result of charge distribution and ring tautomerization. In other words, the conversion of an adjacent carbonyl to a hydroxyl may mimic the behavior of the hydroxyl oxygen in AHA, which acts to stabilize the barbituric ring with the Ni^{2+} ions. Similarly, one of the nitrogen atoms in the barbituric ring coordinates with one

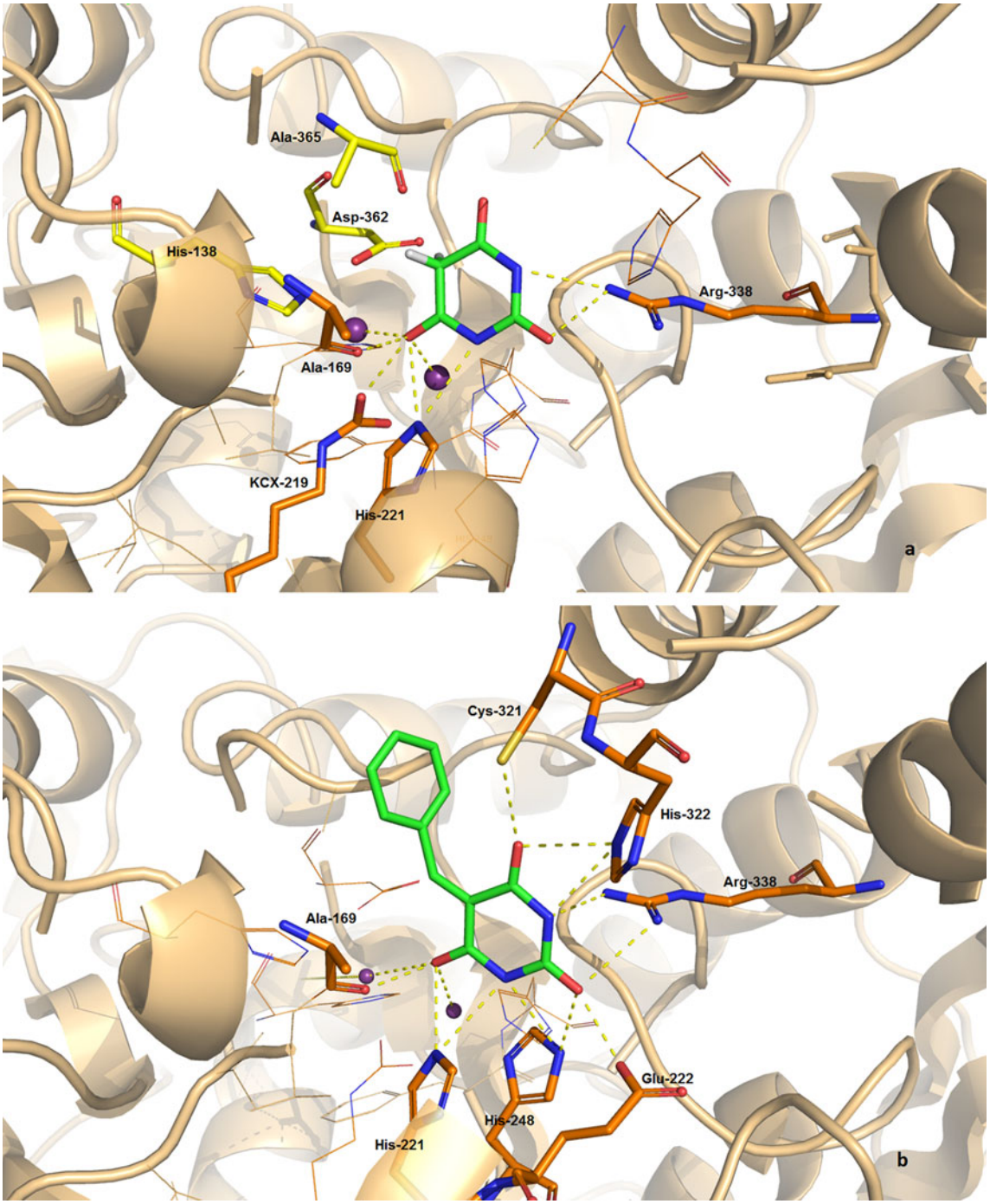

Fig. 5 Interactions of barbituric acid (*left*) and 5-benzylidene barbituric acid (*right*) with the active site of *H. pylori* urease. The compounds and H-bonding residues are represented by *sticks*, and the Ni^{2+} ions are represented by *balls.* The residues surrounding 2(H)–Cα are shown in a *yellow color*

of the nickel ions, which is reminiscent of the behavior of the carbonyl oxygens in the AHA. Thus, we can propose that this compound mimics the binding mode of AHA. Six hydrogen bonds are also formed between the barbituric acid and important active site residues; R338 (NH_2), H321 (NE), A169 (C=O), and KCX 219 (OQ2).

In addition, special attention was directed to the fact that compounds with a hydrophobic arylidene group showed enhanced potency with respect to urease inhibition. This is because the active site of urease is located within an internal cavity and is surrounded by hydrophobic amino acid residues of the urease enzyme. The hydrophobic character of the R moiety of the barbituric acid derivative plays a role in the hydrophobic binding near the active site of urease. We can see that unsubstituted 5-benzylidene barbiturate (**1a**) is more active, with an IC_{50} value of 41.6 μM, than the others.

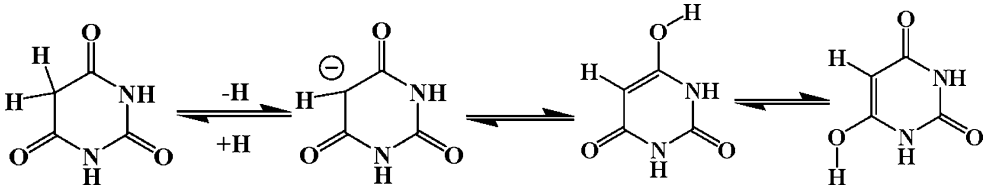

Fig. 6 Representation of the aromatic stabilization and tautomerization of barbituric acid

This finding is compatible with the results of a previous study by Tanaka et al., which indicated that R moieties of hydroxyketone with hydrophobic character potentiate urease inhibition in this class [23].

Upon further inspection, we noted that there is a hydrophobic environment around the active site of urease (Fig. 7). A hydrophobic pocket is created by amino acid residues such as M366 and A365 as part of the nearest loop and M317, L318, M319, C321, and V320 as part of two separate helices, and the presence of these residues helps explain why compound **1a** with an arylidene group has stronger biological activity than barbituric acid.

Additionally, Table 2 shows that *para*-substituted 5-benzylidene barbiturates have lower docking energies than other analogs. To investigate the reason for this result, we generated Fig. 8. This shows that N168 and M366 orient towards the *ortho* (b and c) and *meta* (b′ and c′) positions on the aryl part of 5-benzylidene barbituric acid (**1a**) and cause spatial repulsion, whereas the *para* position, which is not surrounded by any residues, can tolerate substituents ranging from small (F) to rather bulky ($-OCH_3$) in size.

It is interesting to examine the docking poses shown in Fig. 9 in detail. It shows that substitution at the *ortho* and *meta* positions of the aryl part keeps the metal-coordinating barbituric ring far from the nickel ions, thus decreasing the tendency of these compounds to coordinate. Based on the docking results, although the *ortho* and *meta* substituted 5-benzylidene barbituric acid derivatives (**1b** and **1c**) fitted well into the binding pocket, another docking pose was observed for them, in which there is arene–cation interaction between the phenyl ring and one of the nickel ions. The barbituric ring stacks between H221 and H248. In addition, the hydroxyl and nitro groups of compounds **1b** and **1c** present hydrogen bonding with R338. These weak interactions with the binding pocket of urease might be one of the reasons for the higher docking energies exhibited by these compounds (**1b–c**).

A number of investigators have postulated that antibacterial agents increase the rate and efficiency of growth in animals and birds by suppressing the production of toxic substances by gastrointestinal bacteria [24]. Ammonia was

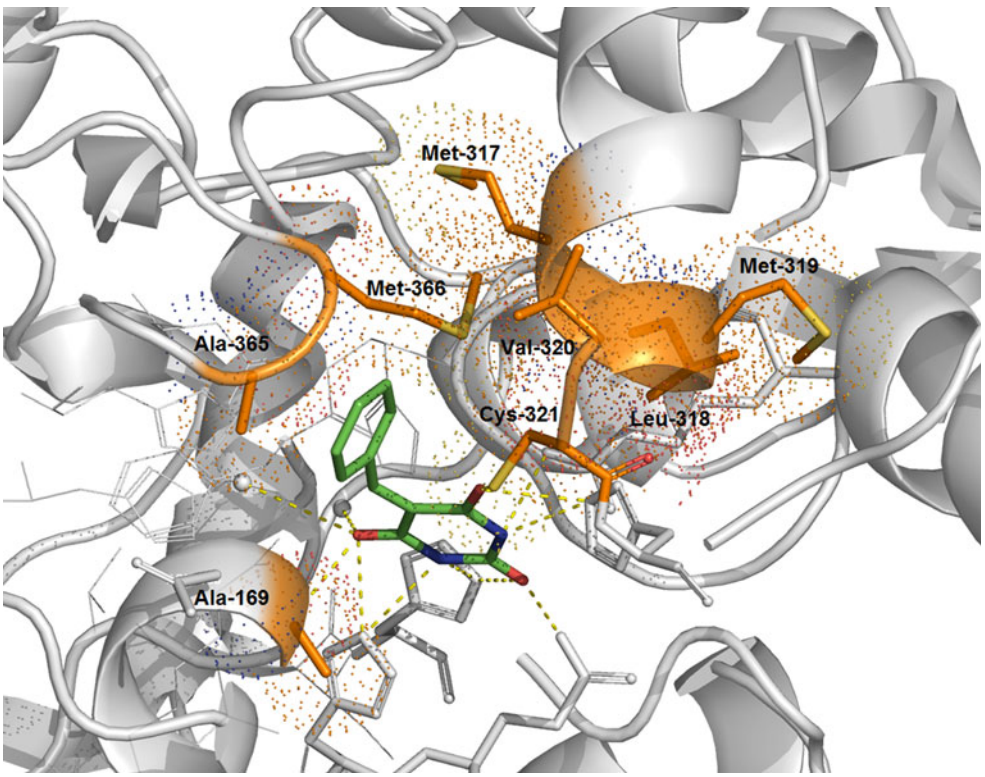

Fig. 7 Hydrophobic pocket around the active site of urease, as shown by the *orange color* and *dots*

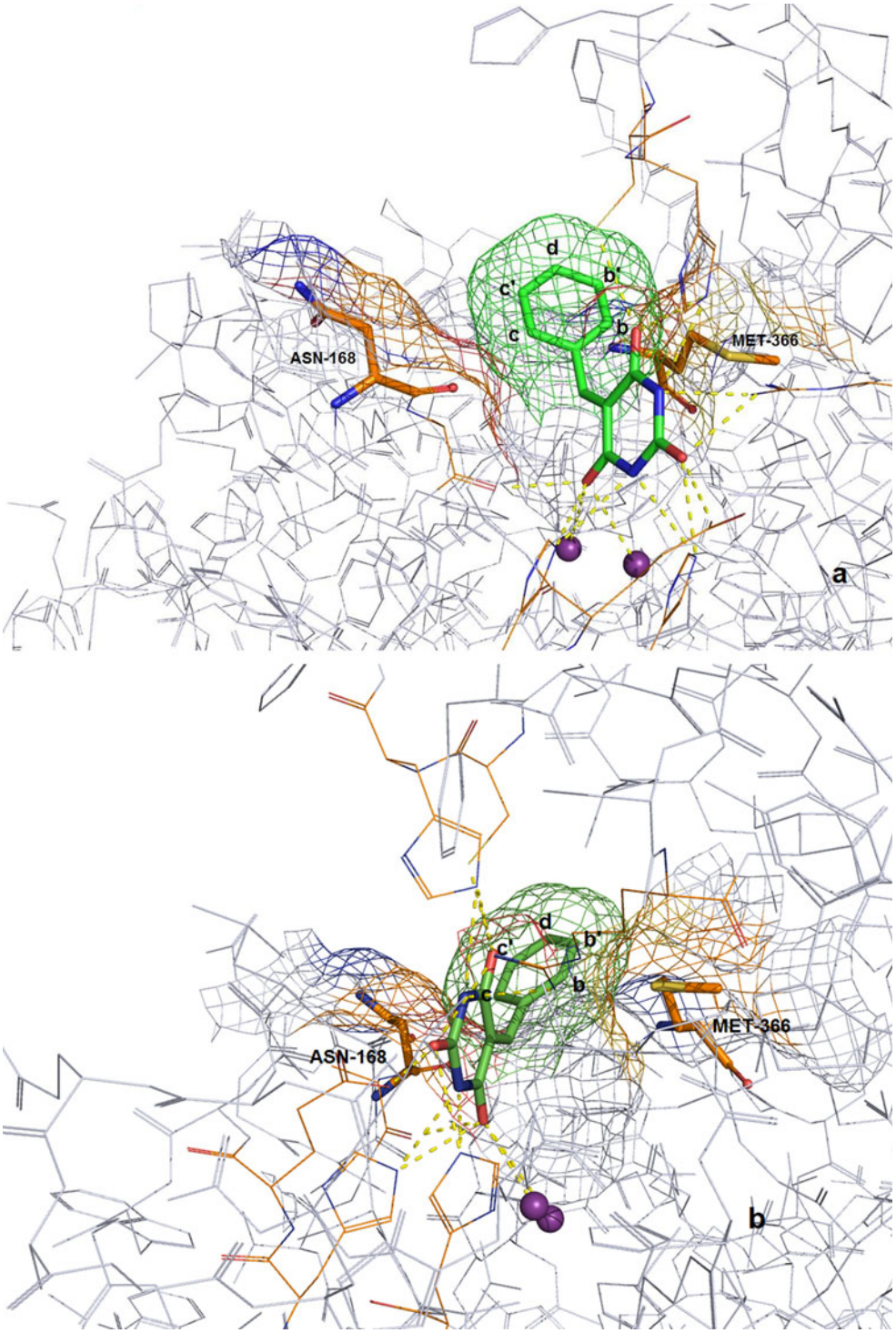

Fig. 8 Mesh representation of the surroundings of 5-benzylidene barbituric acid. ASN-168 is in close contact with the positions c and c′ on arylidene through its C=O group and Cβ in **a**, and Met-366 makes close contact with b and b′ through its S and Cγ, respectively, in **b**

suggested to be one of these toxins, and urease is the source of ammonia production.

The discovery that barbituric acid inhibits urease was made by Gray et al., who observed that certain cyclic urea compounds (i.e., barbituric and thiobarbituric acids) were capable of inhibiting bacterial and jack-bean urease [25, 26].

The effects of barbituric acid on gastrointestinal ammonia concentration and urease activity were also presented by Visek et al. and Harbers et al., who reported a reduction in intestinal ureolytic activity with barbituric acid in rat and chicks fed with carbohydrate [27, 28]. In preliminary work by Harbers et al., ammonia production and urea hydrolysis in the gastrointestinal tracts of casein-fed birds were found

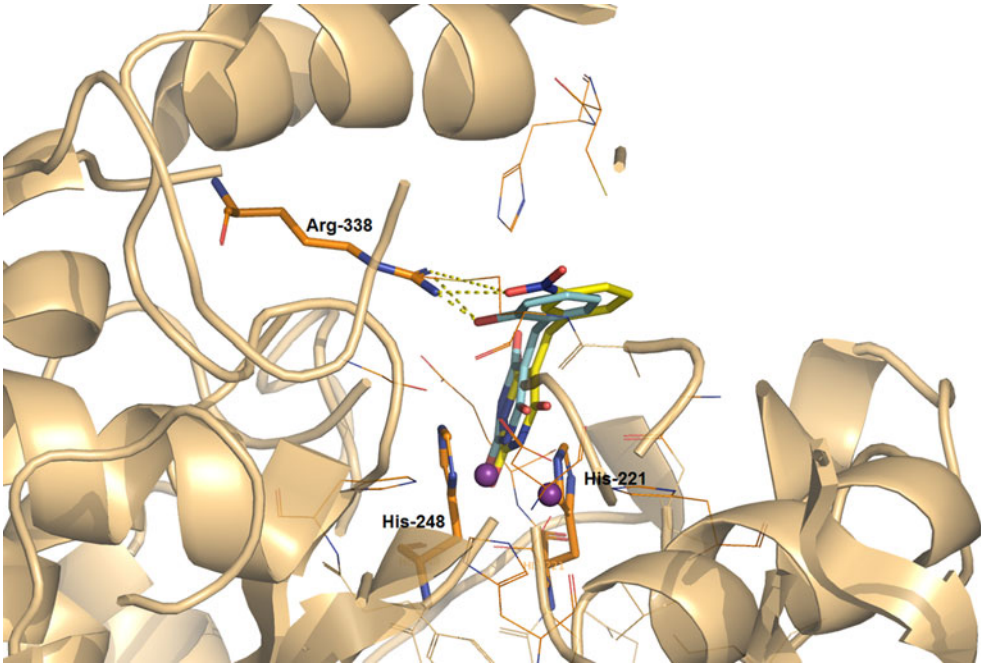

Fig. 9 Interactions of compounds **1b** (*blue*) and **1c** (*yellow*) with the active site of *H. pylori* urease. Key residues are shown as *sticks*

to be suppressed upon feeding chicks for four weeks with a purified diet supplemented with barbituric acid, thus indicating that reducing the level of ammonia (a toxic compound) improved chick growth and weight gain [29]. A similar study was conducted by Clifford et al. in 1968, which determined the effects of several urease inhibitors such as barbituric acid, copper, and nitrate ion on the growth and metabolism of sheep and cattle fed urea-containing diets [30]. However, conversely, none of these inhibitors affected lamb growth when they were included at three different levels in high- or low-grain diets.

Following the work of Gary et al. [26], Rauf et al. reported that some barbituric and thiobarbituric acid derived sulfonamides were urease inhibitors [31]. Recently, Khan et al. investigated the urease inhibitory activities of arylidene barbiturates as a novel class of radical scavengers [32]. Analysis of the docking results showed that, in most of the molecules, one of the carbonyl groups coordinated with both nickel atoms, while the other was involved in the formation of hydrogen bonds with important active-site residues. This is in accord with our results, in which D362, A365, and H138 were found to have the potential to abstract the acidic hydrogen of the α-carbon and produce an ionizable barbituric ring, meaning that carbonyls adjacent to the α-carbon have the potential to change into hydroxyls as a result of charge distribution and ring tautomerization; such carbonyl groups can coordinate with the nickel ion. We also found that hydrogen bonds formed between barbituric acid and important active site residues: R338 (NH_2), H321 (NE), A169 (C=O), and KCX 219 (OQ2). In addition, Khan et al. showed that *para*-substituted barbiturates are more potent inhibitors than *ortho* and *meta* analogs, which is in agreement with the results of our docking study, which indicated that the *para* position is free of repulsion from neighboring residues, so it can better tolerate a substituent than the other positions.

Conclusions

In summary, we carried out a virtual screening of the ZINC database in order to find novel urease inhibitors. Structure-based virtual screening and molecular docking were employed to further screen the compounds. Using this approach, a novel class of urease inhibitors was successfully identified with an acceptable correlation between biological activities and binding energies, and the potencies of the members of this class are greater than that of hydroxyurea. Barbituric acid and its derivatives (**1a–h**) have the potential to inhibit urease. 5-Benzylidene barbituric acid presents a stronger biological activity than barbituric acid.

Furthermore, these results suggest that among the substituted 5-benzylidene barbiturates, those with *para* substitution have higher urease inhibition activities than those with *meta* or *ortho* substitution. This may be because the barbituric acid moiety is closer to the bimetallic nickel center in unsubstituted or *para*-substituted analogs than in *ortho*- or *meta*-substituted analogs, so it has greater chelating ability. The results presented here lead us to conclude that these compounds can be used as starting points for lead optimization.

Acknowledgments The authors would like to thank the Research Council of Tehran University of Medical Sciences and the Iranian National Science Foundation (INSF) for providing the financial support for this work.

References

1. Covacci A, Telford LJ, Giudice GD, Parsonnet J, Rappuoli R (1999) *Helicobacter pylori* virulence and genetic geography. Science 284:1328–1333
2. Amieva MR, El-Omar EM (2008) Host-bacterial interactions in *Helicobacter pylori* infection. Gastroenterology 134:306–323
3. Krajewska B (2009) Ureases. I. Functional, catalytic and kinetic properties: a review. J Mol Catal B Enzym 59:9–21
4. Andersen LP (2007) Colonization and infection by *Helicobacter pylori* in humans. Helicobacter 12:12–15
5. Mobley HL, Island MD, Hausinger RP (1995) Molecular biology of microbial ureases. Microbiol Rev 59:451–480
6. Krajewska B (2002) Ureases: roles, properties and catalysis. Wiad Chem 56:223–253
7. Ha NC, Oh ST, Sung JY, Cha KA, Lee MH, Oh BH (2001) Supramolecular assembly and acid resistance of *Helicobacter pylori* urease. Nat Struct Biol 8:505–509
8. Ciurli S, Benini S, Rypniewski WR, Wilson KS, Miletti S, Mangani S (1999) Structural properties of the nickel ions in urease: novel insights into the catalytic and inhibition mechanisms. Coord Chem Rev 190:331–355
9. Farber GK (1999) New approaches to rational drug design. Pharmacol Ther 84:327–332
10. Amtul Z, Atta-ur-Rahman SAR, Choudhary IM (2002) Chemistry and mechanism of urease inhibition. Curr Med Chem 9:1323–1348
11. Azizian H, Bahrami H, Pasalar P, Amanlou M (2010) Molecular modeling of *Helicobacter pylori* arginase and the inhibitor coordination interactions. J Mol Graph Mod 28:626–635
12. Musiani F, Arnofi E, Casadio R, Ciurli S (2001) Structure-based computational study of the catalytic and inhibition mechanisms of urease. J Biol Inorg Chem 6:300–314
13. Bas DC, Rogers DM, Jensen JH (2008) PROPKA, very fast prediction and rationalization of pK_a values for protein–ligand complexes. Proteins 73:765–783
14. Irwin JJ, Shoichet BK (2005) ZINC: a free database of commercially available compounds for virtual screening. J Chem Inf Comput Sci 45:177–182
15. Lipinski CA, Lombardo F, Dominy BW, Feeney PJ (2001) Experimental and computational approaches to estimate solubility and permeability in drug discovery and development settings. Adv Drug Del Rev 46:3–26
16. Morris GM, Goodsell DS, Halliday RS, Huey R, Hart WE, Belew RK, Olson AJ (1998) Automated docking using a Lamarckian genetic algorithm and an empirical binding free energy function. J Comput Chem 19:1639–1662
17. Sanner MF (1999) Python: a programming language for software integration and development. J Mol Graph Model 17:57–61
18. Weatherburn MW (1967) Phenol–hypochlorite reaction for determination of ammonia. Anal Chem 39:971–974
19. Nabati F, Habibi-Rezaei M, Amanlou M, Moosavi-Movahedi AA (2011) Dioxane enhanced immobilization of urease on alkyl modified nano-porous silica using reversible denaturation approach. J Mol Catal B Enz 70:17–22
20. Mohit LD, Pulak JB (2005) Uncatalysed Knoevenagel condensation in aqueous medium at room temperature. Tetrahedron Lett 46:6453–6456
21. Peet NP, Sunder S, Barbuch RJ, Vinogradoff AP (1986) Mechanistic observation in the Gewald syntheses of aminothiophens. J Heterocycl Chem 23:129–134
22. Khan KM, Wadood A, Ali M, Zia-Ullah Ul-Haq Z, Lodhi MA, Khan M, Perveen S, Choudhary MI (2010) Identification of potent urease inhibitors via ligand- and structure-based virtual screening and in vitro assays. J Mol Graph Model 28:792–798
23. Tanaka T, Kawase M, Tani S (2004) Alpha-hydroxyketones as inhibitors of urease. Bioorg Med Chem 12:501–505
24. Dintzis RZ, Hastings AB (1953) The effect of antibiotics on urea breakdown in mice. Proc Natl Acad Sci USA 39:571–578
25. Gray CT, Brooke MS, Gerhart JC (1959) Inhibition of urease by alloxan and alloxanic acid. Nature 184:1936–1937
26. Gary CT, Brooke MS, Gerhart JC (1961) Metabolism of alloxanic acid in soil microorganism. J Bacteriol 81:755–761
27. Visek WJ, Baron JM, Switz DM (1959) Urea metabolism and intestinal ureolytic activity of rats fed antimicrobial agents. J Pharm Exp Therap 126:359–365
28. Harbers LH, Alvares AP, Jacobsen AI, Visek WJ (1962) Growth of chicks fed diets supplemented with chlortetracycline or barbituric acid. Fed Prec Abstr 21:386
29. Alvares AP, Harbers LH, Visek WJ (1962) Effect of barbituric acid, chlortetracycline and carbohydrates upon growth and gastrointestinal urease activity of chicks. J Nutr 82:93–98
30. Clifford J, Bourdette JR, Tillman AD (1968) Effect of urease inhibitors on sheep fed diets containing urea. J Anim Sci 27:1073–1080
31. Rauf A, Ahmed F, Qureshi AM, Aziz-ur-Rehman KA, Qadir MI, Choudhary MI, Chohan ZH, Youssoufid MH, Ben Haddad T (2011) Synthesis and urease inhibition studies of barbituric and thiobarbituric acid derived sulphonamides. J Chin Chem Soc 58:1–10
32. Khan KM, Ali M, Wadood A, Ul-Haq Z, Zia-Ullah KM, Lodhi MA, Perveen S, Choudhary MI, Volter W (2011) Molecular modeling-based antioxidant arylidene barbiturates as urease inhibitors. J Mol Graph Model 30:153–156